Steady-State Solution of the Euler Equations for Transonic Flow

A. Jameson

1. Introduction

The most important requirement for aeronautical applications of computational methods in fluid dynamics is the capability to predict the steady flow past a proposed configuration, so that key performance parameters such as the lift to drag ratio can be estimated. Even in maneouvering flight the time scales of the motion are large compared with those of the flow, so that unsteady effects are secondary. Thus the aerodynamic design will normally be based on analysis of steady flow. In fact unsteady flow due to buffet or wing flutter is not acceptable for normal operation, so the analysis of unsteady flow is required primarily for checking the structural integrity at the limits of the flight envelope, such as establishing that the minimum speed at which flutter can occur is greater than the maximum permissible speed in a dive. It is particularly important to be able to calculate steady solutions of aerodynamic flows in the transonic range, where the formation of shock waves leads to the onset of drag rise, and a drastic deterioration of the lift to drag ratio as the speed of the airplane approaches the speed of sound.

Transonic, Shock, and Multidimensional Flows:
Advances in Scientific Computing

ISBN 0-12-493280-0

In the last decade revolutionary progress has been made in our ability to predict complex transonic flows past wings and wing-body combinations[1-4]. Most of this work has rested on the assumption of potential flow, which allows the Euler equations to be reduced to a single second order partial differential equation of mixed type for the potential. As the Mach number is increased and the shock waves become strong enough to produce appreciable amounts of entropy and vorticity, the assumption of potential flow becomes progressively less acceptable. Some disturbing discrepancies between potential flow solutions and solutions of the Euler equations have been noted at quite moderate Mach numbers, such as the NACA 0012 airfoil at Mach .8 and an angle of attack of 1.25°[5]. Some non-unique solutions of the potential equation have also been discovered for flows containing fairly strong shock waves[6], raising the question of whether the Euler equations admit a similar non-uniqueness, and whether these solutions are stable solutions of the time dependent equations. There are also engineering applications where the flow is essentially rotational. For example, there is renewed interest in the use of propellers to increase the propulsive efficiency of long range transport aircraft. This leads to the requirement to predict the flow over a wing in a swirling slipstream behind a propeller. Thus there is a real need for an efficient method of calculating steady solutions of the Euler equations without introducing the assumption of potential flow.

The conditions for the existence and uniqueness of a steady state solution of the Euler equations are not well established. It is, however, an accepted practice to integrate the time dependent Euler equations until the solution approaches a steady state.[7-9] For the case of a flow in a domain exterior to a body, one anticipates that a steady state will be reached by the propagation of disturbances to infinity. This paper focusses on ways to increase the efficiency of this procedure. The following questions

are addressed in particular:

1. The choice of an efficient time stepping procedure to maximize the amount by which the solution can be advanced in time for a given amount of computational effort.
2. The choice of dissipative terms to prevent undesired oscillations in the solution.
3. The treatment of the boundary conditions in the far field to reduce reflection of waves back into the flow field.
4. Acceleration of the rate of convergence to a steady state by artificial modifications of the time dependent equations.

The work has been conducted in cooperation with Wolfgang Schmidt* and Eli Turkel†

2. Finite Volume Scheme for Space Discretization

Since the emphasis is on steady state solutions, it is convenient to formulate the space and time discretization procedures separately, in such a way that the steady state solution is independent of the time step, so that very large time steps can be used without altering the solution. The scheme must be able to represent the stationary shock waves which can be expected to appear in a steady transonic flow. For the present purpose, however, the ability to simulate travelling wave fronts without distortion over long periods of time, as might be needed, for example, for a Riemann problem, is of secondary importance, as long as the final steady state solution is unimpaired. It turns out that it is not necessary to resort to upwind differencing and flux vector splitting[10,11]. Quite satisfactory representations of stationary shock waves can be provided by the use of a comparatively simple central difference scheme, augmented by the addition of dissipative terms with a magnitude determined by local flow gradients.

---

* Dornier Gmbh, Friedrichshafen.

† University of Tel Aviv, Israel.

In order to provide the flexibility to treat arbitrary geometric configurations a finite volume formulation is used for the space discretization. Let p, ρ, u, v, E and H denote the pressure, density, Cartesian velocity components, total energy and total enthalpy. For a perfect gas

$$E = \frac{p}{(\gamma-1)\rho} + \frac{1}{2}(u^2+v^2), \quad H = E + \frac{p}{\rho} \tag{1}$$

where γ is the ratio of specific heats. The Euler equations for two dimensional inviscid flow can be written in integral form for a region Ω with boundary $\partial\Omega$ as

$$\frac{\partial}{\partial t}\iint_{\Omega} w \, dx \, dy + \oint_{\partial\Omega} (f dy - g dx) = 0 \tag{2}$$

where x and y are Cartesian coordinates and

$$w = \begin{pmatrix} \rho \\ \rho u \\ \rho v \\ \rho E \end{pmatrix}, \quad f = \begin{pmatrix} \rho u \\ \rho u^2+p \\ \rho uv \\ \rho uH \end{pmatrix}, \quad g = \begin{pmatrix} \rho v \\ \rho vu \\ \rho v^2+ p \\ \rho vH \end{pmatrix} \tag{3}$$

The computational domain is divided into quadrilateral cells as in the sketch, and a system of ordinary differential equations is obtained by applying equation (2) to each cell separately. The resulting equations can then be solved by several alternative time stepping schemes.

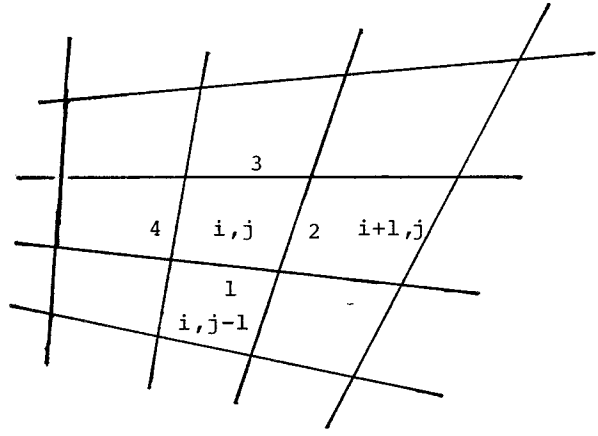

Let the values of the quantities associated with each cell be denoted by subscripts i, j. (These can be regarded as values at the cell center, or average values for the cell). For each cell equation (2) assumes the form

$$\frac{d}{dt}\ (hw) + Qw = 0 \tag{4}$$

where h is the cell area, and the operator Q represents an approximation to the boundary integral in the second term of equation (2). This is defined as follows. Let Δx_k and Δy_k be the increments of x and y along side k of the cell, with appropriate signs. Then the flux balance for, say, the x momentum component, is represented as

$$\frac{\partial}{\partial t}(h\rho u) + \sum_{k=1}^{4} (q_k \rho u_k + \Delta y_k p_k) = 0 \tag{5}$$

where h is the cell area, q_k is the flux velocity

$$q_k = \Delta y_k u_k - \Delta x_k v_k \tag{6}$$

and the sum is over the four sides of the cell. Each quantity such as u_1 or $(\rho u)_1$ is evaluated as the average of the values in the cells on the two sides of the face,

$$(\rho u)_1 = \frac{1}{2}\ (\rho u)_{i,j} + \frac{1}{2}\ (\rho u)_{i,j-1} \tag{7}$$

for example. The scheme reduces to a central difference scheme on a Cartesian grid, and is second order accurate provided that the grid is smooth enough.

3. Dissipative Terms

The finite volume scheme is augmented by the addition of dissipative terms designed to suppress the tendency for odd and even point oscillations, and to limit the generation of wiggles and overshoots near shock waves. The basic

dissipative terms are second differences with a coefficient proportional to the absolute value of the second difference of the pressure. Thus the coefficient is very small except in regions of large pressure gradient, such as the neighborhood of a shock wave or stagnation point. The amount of dissipation provided by these terms proved sufficient to eliminate ripples from the solutions, but the calculations would generally not converge to a completely steady state. Instead, after the flow reached an almost steady state, oscillations of very low amplitude (with max $\frac{\partial \rho}{\partial t} \sim 10^{-3}$, for example) would continue indefinitely. The oscillations had long time periods, as if they were induced by reflections from the boundaries of the computational domain. It turns out that the calculations do converge to a completely steady state when the amount of dissipation in the smooth part of the flow is increased by the introduction of terms containing fourth differences. A fixed coefficient can be used for these terms without impairing the overall order of accuracy of the scheme. Near shock waves, however, the fourth differences tend to induce overshoots. This can be prevented by subtracting the coefficient of the second differences, which becomes large in regions of high pressure gradient, from the coefficient of the fourth differences, so that the terms containing the fourth differences are switched off when the terms containing the second differences are switched on.

This leads to the following scheme: equation (4) is replaced by the equation

$$\frac{d}{dt}(hw) + Qw - Dw = 0 \tag{8}$$

where Q is the spatial discretization operator defined by equations (5-7), and the operator D introduces the dissipative terms. For the density equation

$$D\rho = D_x\rho + D_y\rho \tag{9}$$

where $D_x\rho$ and $D_y\rho$ are corresponding contributions for the two coordinate directions, written in conservation form

$$D_x\rho = d_{i+\frac{1}{2},j} - d_{i-\frac{1}{2},j} \tag{10}$$

$$D_y\rho = d_{i,j+\frac{1}{2}} - d_{i,j-\frac{1}{2}}$$

The terms on the right all have a similar form:
for example

$$d_{i+\frac{1}{2},j} = \frac{h_{i+\frac{1}{2},j}}{\Delta t}\left\{ \begin{array}{l} \varepsilon^{(2)}_{i+\frac{1}{2},j}\ (\rho_{i+1,j} - \rho_{i,j}) \\ \\ -\varepsilon^{(4)}_{i+\frac{1}{2},j}\ (\rho_{i+2,j} - 3\rho_{i+1,j} + 3\rho_{i,j} - \rho_{i-1,j}) \end{array} \right\} \tag{11}$$

where h is the cell volume, and the coefficients $\varepsilon^{(2)}$ and $\varepsilon^{(4)}$ are adapted to the flow. Define

$$\nu_{i,j} = \left| \frac{p_{i+1,j} - 2p_{i,j} + p_{i-1,j}}{p_{i+1,j} + 2p_{i,j} + p_{i-1,j}} \right| \tag{12}$$

Then

$$\varepsilon^{(2)}_{i+\frac{1}{2},j} = \kappa^{(2)} \max\ (\nu_{i+1,j},\ \nu_{i,j}) \tag{13}$$

and

$$\varepsilon^{(4)}_{i+\frac{1}{2},j} = \max \left\{ 0,\ (\kappa^{(4)} - \varepsilon^{(2)}_{i+\frac{1}{2},j}) \right\} \tag{14}$$

where typical values of the constants $\kappa^{(2)}$ and $\kappa^{(4)}$ are

$$\kappa^{(2)} = \frac{1}{4}\ ,\ \kappa^{(4)} = \frac{1}{256}$$

The dissipative terms for the remaining equations are obtained by substituting ρu, ρv and either ρE or ρH for ρ in these formulas.

The scaling $h/\Delta t$ in equation (11) conforms to the inclusion of the cell area h in the dependent variables of equation (8). Since equation (11) contains undivided differences, it follows that if $\varepsilon^{(2)} = O(\Delta x^2)$ and $\varepsilon^{(4)} = O(1)$, then the added terms are of order Δx^3. This will be the case in a region where the flow is smooth. Near a shock wave $\varepsilon^{(2)} = O(1)$, and the scheme behaves locally like a first order accurate scheme.

4. Time Stepping Schemes

The objective of the time stepping procedure is to advance the solution to a steady state as rapidly as possible for a given amount of computational effort. The use of an implicit scheme permits a larger time step but requires more effort per time step. To keep the operation count for each step within reasonable bounds one has to resort to some kind of factorization, such as that of Beam and Warming[12]. When the time step Δt becomes large the factorization is then dominated by terms of order Δt^2, so that the optimal step for convergence to a steady state is not necessarily as large as all that. The present investigation concentrates on the use of explicit schemes which allow relatively large time steps. These have the advantage that they are readily amenable to vectorization, so that the resulting code can take full advantage of the power of vector computers such as the Cray 1 or Cyber 205. Multistage two level schemes of the Runge-Kutta type have the advantage that they do not require any special starting procedure, in contrast to leap frog and Adams-Bashforth methods, for example. The extra stages can be used either

(1) to improve accuracy, or

(2) to extend the stability region.

An advantage of this approach is that the properties of

these schemes have been widely investigated, and are readily available in textbooks on ordinary differential equations.

In the present case, if the grid is held fixed in time so that the cell area h is constant, the system of equations (8) has the form

$$\frac{dw}{dt} + Pw = 0 \tag{15}$$

where if Q is the discretization operator defined in Section 2, and D is the dissipative operator defined in Section 3, the nonlinear operator P is defined as

$$Pw \equiv \frac{1}{h} (Qw - Dw) \tag{16}$$

The investigation has concentrated on two time stepping schemes. The first is a three stage scheme which is defined as follows. Let a superscript n denote the time level, and let Δt be the time step. Then at time level n set

$$\begin{aligned} w^{(0)} &= w^n \\ w^{(1)} &= w^{(0)} - \Delta t\, Pw^{(0)} \\ w^{(2)} &= w^{(0)} - \frac{\Delta t}{2} (Pw^{(0)} + Pw^{(1)}) \\ w^{(3)} &= w^{(0)} - \frac{\Delta t}{2} (Pw^{(0)} + Pw^{(2)}) \\ w^{n+1} &= w^{(3)} \end{aligned} \tag{17}$$

Variations of this scheme have been proposed by Gary[13], Stetter[14], and Graves and Johnson[15]. It can be regarded as a Crank-Nicolson scheme with a fixed point iteration to determine the solution at time level n+1, and the iterations terminated after the third iteration. It is second order accurate in time, and for the model problem

$$u_t + au_x = 0 \quad , \quad u(x,0) \text{ given} \tag{18}$$

it is stable when the Courant number

$$\left| a \frac{\Delta t}{\Delta x} \right| \leq 2$$

This bound is not increased by additional iterations. Compared with standard third order Runge-Kutta schemes, this scheme gives up third order accuracy in time in favor of a larger bound on the Courant number.

The other scheme which has been extensively investigated is the classical fourth order Runge-Kutta scheme, defined as follows. At time level n set

$$\begin{aligned}
w^{(0)} &= w^n \\
w^{(1)} &= w^{(0)} - \frac{\Delta t}{2} Pw^{(0)} \\
w^{(2)} &= w^{(0)} - \frac{\Delta t}{2} Pw^{(1)} \\
w^{(3)} &= w^{(0)} - \Delta t\, Pw^{(2)} \\
w^{(4)} &= w^{(0)} - \frac{\Delta t}{6} (Pw^{(0)} + 2Pw^{(1)} + 2Pw^{(2)} + Pw^{(3)}) \\
w^{n+1} &= w^{(4)}
\end{aligned} \tag{19}$$

This scheme is fourth order accurate in time, and for the model problem (18) it is stable for Courant numbers

$$\left| \frac{a\Delta t}{\Delta x} \right| \leq 2\sqrt{2}$$

Its stability region, which is displayed on page 176 of Ref. (16), for example, also extends well to the left of the imaginary axis, allowing latitude in the introduction of dissipative terms.

Both schemes have the property that if $Pw^n = 0$ then $w^{(1)} = w^{(0)}$, and so on, so that $w^{n+1} = w^n$, and the steady state solution is

$$Pw = 0$$

independent of the time step Δt. This allows a variable time step determined by the bound on the local Courant number to be used to accelerate convergence to a steady state without altering the steady state.

The expense of re-evaluating the dissipative terms at every stage of these schemes is substantial. One method of avoiding this is to introduce the dissipative terms in a separate fractional step after the last stage of the Runge-Kutta scheme. Thus equation (16) is replaced by

$$Pw \equiv \frac{1}{h} Qw \tag{16*}$$

and the fourth order Runge Kutta scheme defined by equation (19), for example, is modified by setting

$$w^{n+1} = w^{(4)} + \Delta t D\, w^{(4)}$$

This method has the advantage that the stability properties for the two fractional steps are independent, so that the scheme will be stable if each fractional step is stable. It has the disadvantage that the steady state solution is no longer independent of the time step.

An alternative approach which has proved successful in practice, is to freeze the dissipative terms at their values in the first stage. Thus the fourth order Runge-Kutta scheme is modified so that it has the form

$$\begin{aligned}
w^{(0)} &= w^{n} \\
w^{(1)} &= w^{(0)} - \frac{\Delta t}{2h} Qw^{(0)} + \frac{\Delta t}{2h} Dw^{(0)} \\
w^{(2)} &= w^{(0)} - \frac{\Delta t}{2h} Qw^{(1)} + \frac{\Delta t}{2h} Dw^{(0)} \\
w^{(3)} &= w^{(0)} - \frac{\Delta t}{h} Qw^{(2)} + \frac{\Delta t}{h} Dw^{(0)} \\
w^{(4)} &= w^{(0)} - \frac{\Delta t}{6h} (Qw^{(0)} + 2Qw^{(1)} + 2Qw^{(2)} + Qw^{(3)}) \\
&\quad + \frac{\Delta t}{h} Dw^{(0)}
\end{aligned} \tag{20}$$

The operators Q and D require roughly equal amounts of computation. Assigning to each 1 unit of work, and assuming that dissipative terms would be required in the leap frog or MacCormack schemes, both of which have maximum time steps bounded by a Courant number of one, one obtains the following table for the relative efficiency of the schemes:

Scheme	Evaluations of Qw	Evaluations of Dw	Work	Maximum Courant Number	Efficiency = $\frac{\text{time step}}{\text{work}}$
Leap frog	1	1	2	1	1/2
MacCormack	2	1	3	1	1/3
3 stage	3	3	6	2	1/3
4 stage	4	4	8	2.8	.35
4 stage (frozen Dw)	4	1	5	2.8	.56

5. Boundary Conditions

The rate of convergence to a steady state will be impaired if outgoing waves are reflected back into the flow from the boundaries, so it is important to treat the boundary conditions by a method which minimizes wave reflection. Consider first the boundary condition at the profile. Let X and Y be local coordinates such that the boundary coincides with a line Y = constant. Using subscripts X and Y to denote derivatives, the Jacobian

$$h = x_X y_Y - x_Y y_X$$

corresponds to the cell area of the finite volume scheme. In differential form equation (2) then becomes

$$\frac{\partial}{\partial t}(hw) + \frac{\partial}{\partial X}(y_Y f - x_Y g) + \frac{\partial}{\partial Y}(x_X g - y_X f) = 0 \qquad (21)$$

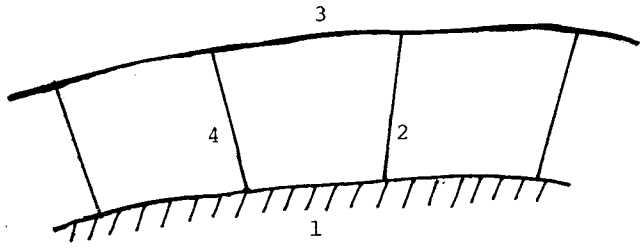

Consider the flux balance for a cell adjacent to the wall, as drawn in the sketch. There is no convected flux across side 1, since

$$x_X v - y_X u = 0 \qquad (22)$$

But there are contributions Δyp and Δxp to the momentum equations, which require an estimate of the pressure at the wall. Taking the time derivative of equation (22) multiplied by ρ, and substituting for $\frac{\partial}{\partial t}(h\rho u)$ and $\frac{\partial}{\partial t}(h\rho v)$ from equation (21) leads to the relation (given by Rizzi[17])

$$(x_X^2 + y_X^2)p_Y = (x_X x_Y + y_X y_Y)p_X + \rho(y_Y u - x_Y v)(vx_{XX} - uy_{XX}) \qquad (23)$$

Thus we can estimate p_Y in terms of quantities which can be determined from the interior solution, and we can use this value of p_Y to extrapolate the pressure from the adjacent cell center to the wall.

In order to treat the flow exterior to a profile one must introduce an artificial outer boundary to produce a bounded domain. If the flow is subsonic at infinity, there will be three incoming characteristics where there is inflow across the boundary, and one outgoing characteristic, corresponding to the possibility of escaping acoustic waves. Where there is outflow, on the other hand, there will be three outgoing characteristics and one incoming characteristic. According to the theory of Kreiss[18], three conditions may therefore be specified at inflow, and one at outflow, while the remaining conditions are determined by the solution of the differential equation. Stable boundary conditions have been given by Gottlieb and Turkel[19] and Gustafsson and Oliger[20] for a variety of difference schemes. The treatment of the outer boundary condition adopted here follows similar lines. The equations are linearized about values at the end of the previous time step, and the characteristic variables corresponding to outgoing characteristics are then determined by extrapolation from the interior, while the remaining boundary conditions are specified in a manner consistent with the conditions imposed by the free stream.

If q_n and q_t are the velocity components normal and tangential to the boundary, and c is the speed of sound, the characteristic speeds for waves impinging on the boundary are q_n, q_t, q_n-c, and $q_n + c$. Let values at the end of the previous time step be denoted by the subscript o. Then the corresponding characteristic variables of the linearized equations are $p-c_o^2\rho$, q_t, $p-\rho_o c_o q_n$ and $p+\rho_o c_o q_n$.

Let values extrapolated from the interior and free stream values be denoted by the subscripts e and ∞. Then at the inflow boundary we set

$$p - c_o^2\rho = p_\infty - c_o^2\rho_\infty \tag{24a}$$

$$q_t = q_{t_\infty} \tag{24b}$$

$$p - \rho_o c_o q_n = p_\infty - \rho_o c_o q_{n_\infty} \tag{24c}$$

$$p + \rho_o c_o q_n = p_e + \rho_o c_o q_{n_e} \tag{24d}$$

yielding

$$p = \frac{1}{2}\left(p_e + p_\infty + \rho_o c_o (q_{n_e} - q_{n_\infty})\right)$$

$$q_n = q_{n_\infty} + \frac{p - p_\infty}{\rho_o c_o}$$

The density can be determined from (24a). For steady state calculations it can alternatively be determined by specifying that the total enthalpy H has its free stream value.

At the outflow boundary one condition should be specified. If the flow is a parallel stream then $\frac{\partial p}{\partial y} = 0$, so for an open domain

$$p = p_\infty \tag{25}$$

A non-reflecting boundary condition which would eliminate incoming waves is

$$\frac{\partial}{\partial t}(p - \rho_o c_o q_n) = 0 \tag{26}$$

This does not assure (25). Following Rudy and Strikwerda[21], (25) and (26) are therefore combined as

$$\frac{\partial}{\partial t}\,(p - \rho_o c_o q_n) + \beta(p - p_\infty) = 0 \qquad (27)$$

where a typical value of the parameter β is 1/8. The velocity components and energy are extrapolated from the interior.

6. Convergence Acceleration

Two ways of accelerating the rate of convergence to a steady state are

1) to increase the speed at which disturbances are propagated through the domain
2) to introduce terms which cause the disturbances to be damped.

Both have been attempted.

In differential form equation (1) is

$$\frac{\partial w}{\partial t} + \frac{\partial}{\partial x} f(w) + \frac{\partial}{\partial y} g(w) = 0 \qquad (25)$$

In a steady state w should satisfy

$$\frac{\partial}{\partial x} f(w) + \frac{\partial}{\partial y} g(w) = 0$$

In order to modify the speed of wave propagation without altering the steady state one can multiply the terms containing the space derivatives by a matrix M to produce the equation

$$\frac{\partial w}{\partial t} + M\left\{ \frac{\partial}{\partial x} f(w) + \frac{\partial}{\partial y} g(w) \right\} = 0 \qquad (26)$$

In this work M has been restricted to the form λI, where λ is a scalar multiplier. Then one can choose λ so that the equations are advanced at the maximum Courant number permitted by the difference scheme at every point in the domain. This is equivalent to using different time steps at different points. The time stepping schemes of Section 4 are so constructed that the steady state is independent of the local time step. Consequently the time step can be altered from one point to the next without altering the steady state.

As a model for this procedure consider the wave equation in polar coordinates r and θ,

$$\phi_{tt} = c^2\left\{\frac{1}{r}\ \frac{\partial}{\partial r}\ (r\phi_r) + \frac{1}{r^2}\ \phi_{\theta\theta}\right\}$$

Suppose that the wave speed c is proportional to the radius, say $c = \alpha r$. Then

$$\phi_{tt} = \alpha^2\left\{r\ \frac{\partial}{\partial r}\ (r\phi_r) + \phi_{\theta\theta}\right\}$$

This has solutions of the form

$$\phi = \frac{1}{r^n} e^{-\alpha n t}$$

indicating the possibility of exponential decay.

As a model for the introduction of damping consider the telegraph equation

$$\phi_{tt} + \alpha\phi_t = \phi_{xx} + \phi_{yy}$$

Multiplying this equation by ϕ_t, and integrating by parts over all space leads to the relation

$$\frac{\partial P}{\partial t} + \alpha \int_{-\infty}^{\infty}\int_{-\infty}^{\infty} \phi_t^2 \, dxdy = 0$$

where

$$P = \frac{1}{2} \int_{-\infty}^{\infty}\int_{-\infty}^{\infty} (\phi_t^2 + \phi_x^2 + \phi_y^2) \, dxdy$$

Since P is non negative, it must decay if $\alpha > 0$ until $\phi_t = 0$. When relaxation methods are regarded as simulating time dependent equations, it is similarly found that the term containing ϕ_t plays a critical role in determining the rate of convergence[22]. One would therefore like to find a method of introducing a term in the Euler equations which would play a similar role.

Assume for the moment that there are no shock waves, and consider the Euler equations in primitive form:

$$\frac{d\rho}{dt} + \rho \nabla \cdot \underline{q} = 0 \tag{27a}$$

$$\frac{d\underline{q}}{dt} + \frac{1}{\rho}\nabla p = 0 \tag{27b}$$

$$\frac{dH}{dt} - \frac{1}{\rho}\frac{\partial p}{\partial t} = 0 \tag{27c}$$

where $\underline{q}$ is the velocity vector,

$$\frac{d}{dt} \equiv \frac{\partial}{\partial t} + \underline{q} \cdot \nabla$$

and H is the total enthalpy. If h is the specific enthalpy then

$$H = h + \frac{q^2}{2}$$

where q is the magnitude of $\underline{q}$. The scalar product of

equation (27b) with $\underline{q}$ can be subtracted from equation (27c) to give

$$\frac{dh}{dt} + \frac{1}{\rho} \frac{dp}{dt} = 0$$

which implies the isentropic relation

$$dh + \frac{dp}{\rho} = 0$$

along particle paths. An initially hometropic flow therefore remains homentropic. Equation (27b) then becomes

$$\frac{d\underline{q}}{dt} + \nabla h = 0 \qquad (28)$$

Let Γ be the circulation $\oint \underline{q} \cdot \underline{dx}$ around a closed material loop. Equation (28) yields Kelvin's theorem that

$$\frac{d\Gamma}{dt} = \oint \underline{q} \cdot \underline{dq} - \oint \nabla h \cdot \underline{dx} = 0$$

Thus if the flow is initially homentropic and irrotational it remains so. If one now assumes this to be the case, so that

$$\frac{\partial u}{\partial y} = \frac{\partial v}{\partial x}$$

and sets

$$\underline{q} = \nabla \phi$$

where ϕ is a velocity potential, then equation (28) can be integrated to yield the unsteady Bernoulli equation

$$\frac{\partial \phi}{\partial t} + H = H_\infty \qquad (29)$$

where H_∞ is the total enthalpy in the far field.

This suggests that the difference $H-H_\infty$ can serve in the role of ϕ_t. Suppose that the continuity equation (27a) is now modified by the addition of a term containing $H-H_\infty$ so that it becomes

$$\frac{d\rho}{dt} + \rho\nabla\cdot\underline{q} + \alpha\rho(H-H_\infty) = 0 \qquad (30)$$

where α is a damping parameter. Since in a steady flow $H = H_\infty$, the steady state equation remains unaltered. Also, since Kelvin's theorem is a consequence of equations (27b) and (27c), it still holds. Thus a flow without shock waves should remain irrotational and homentropic, and one can still introduce a potential and obtain the unsteady Bernoulli equation.

Now on differentiating equation (29) with respect to time it becomes

$$\phi_{tt} + u\phi_{xt} + v\phi_{yt} + \frac{\partial h}{\partial t} = 0 \qquad (31)$$

But

$$\frac{\partial h}{\partial t} = \frac{c^2}{\rho}\frac{\partial \rho}{\partial t}$$

where c is the speed of sound, so equation (31) can be combined with equation (30) to give the unsteady potential flow equation with a damping term:

$$\phi_{tt} + 2u\phi_{xt} + 2v\phi_{yt} + \alpha c^2\phi_t$$

$$= (a^2 - v^2)\phi_{xx} - 2uv\phi_{xy} + (a^2-v^2)\phi_{yy}$$

This can be reduced to the telegraph equation by introducing moving coordinates $x^1 = x - ut$, $y^1 = y - vt$. Thus at least in subsonic flow the added terms should have the desired damping effect.

When the density equation is combined with the momentum equations to yield a system of equations in conservation form, the modified equations become

$$\frac{\partial}{\partial t}\rho + \frac{\partial}{\partial x}(\rho u) + \frac{\partial}{\partial y}(\rho v) + \alpha\,\rho(H-H_\infty) = 0 \tag{32a}$$

$$\frac{\partial}{\partial t}(\rho u) + \frac{\partial}{\partial x}(\rho u^2+p) + \frac{\partial}{\partial y}(\rho vu) + \alpha\,\rho u(H-H_\infty) = 0 \tag{32b}$$

$$\frac{\partial}{\partial t}(\rho v) + \frac{\partial}{\partial x}(\rho uv) + \frac{\partial}{\partial y}(\rho v^2+p) + \alpha\,\rho v(H-H_\infty) = 0 \tag{32c}$$

$$\frac{\partial}{\partial t}(\rho E) + \frac{\partial}{\partial x}(\rho uH) + \frac{\partial}{\partial y}(\rho vH) + \alpha\,\rho H(H-H_\infty) = 0 \tag{32d}$$

The energy equation now has a quadratic term in H, like a Riccati equation. This can be destabilizing, and an alternative which has been found effective in practice is to modify the energy equation to the form

$$\frac{\partial}{\partial t}(\rho E) + \frac{\partial}{\partial x}(\rho uH) + \frac{\partial}{\partial y}(\rho vH) + \alpha(H-H_\infty) = 0$$

which tends to drive H towards H_∞.

7. Results

The ideas developed in Sections 2-6 have been extensively tested in numerical experiments. Some results are presented here for nonlifting flows past a circular cylinder and an NACA 0012 airfoil. Because of the symmetry the calculations were restricted to the flow in the upper half plane. Polar coordinates were used for the cylinder. An O mesh was generated for the NACA 0012 airfoil by transforming the profile to a near circle by a Joukowski transformation, shearing the near circle to a circle, and then mapping polar coordinates in the domain exterior to the circle back to the physical plane by reversing the Joukowski transformation. In each case the mesh contained 64 intervals in the chordwise direction, and 32 intervals in the normal direction, extending to a distance of about 25 chords from the profile, with a mesh interval near the outer boundary of about a chord. In the case of the NACA 0012 airfoil the cells adjacent to the outer boundary had an area 25 million times greater than the area of the smallest cell, adjacent to the trailing edge. The numerical experiments confirmed that the modified four stage Runge-Kutta scheme defined by equation (20) was more efficient than the other schemes, and this scheme was used to produce all the results displayed in this section.

Figures 1 and 2 show results for a circular cylinder at Mach .35 and Mach .45. Each figure shows the computed pressure distribution and the convergence history of the calculation. The flow is fully subsonic in the first case, and there should be no departure from fore and aft symmetry if the calculation were exact. The flow should also be isentropic. The calculations were normalized with $p = 1$ and $\rho = 1$ at infinity, so the quantity $S = p/\rho^{\gamma} - 1$ can be used as a measure of entropy generation. The maximum computed value of S was .0003. At Mach .45 there is a moderately strong shock wave, as can be seen in Figure 2a.

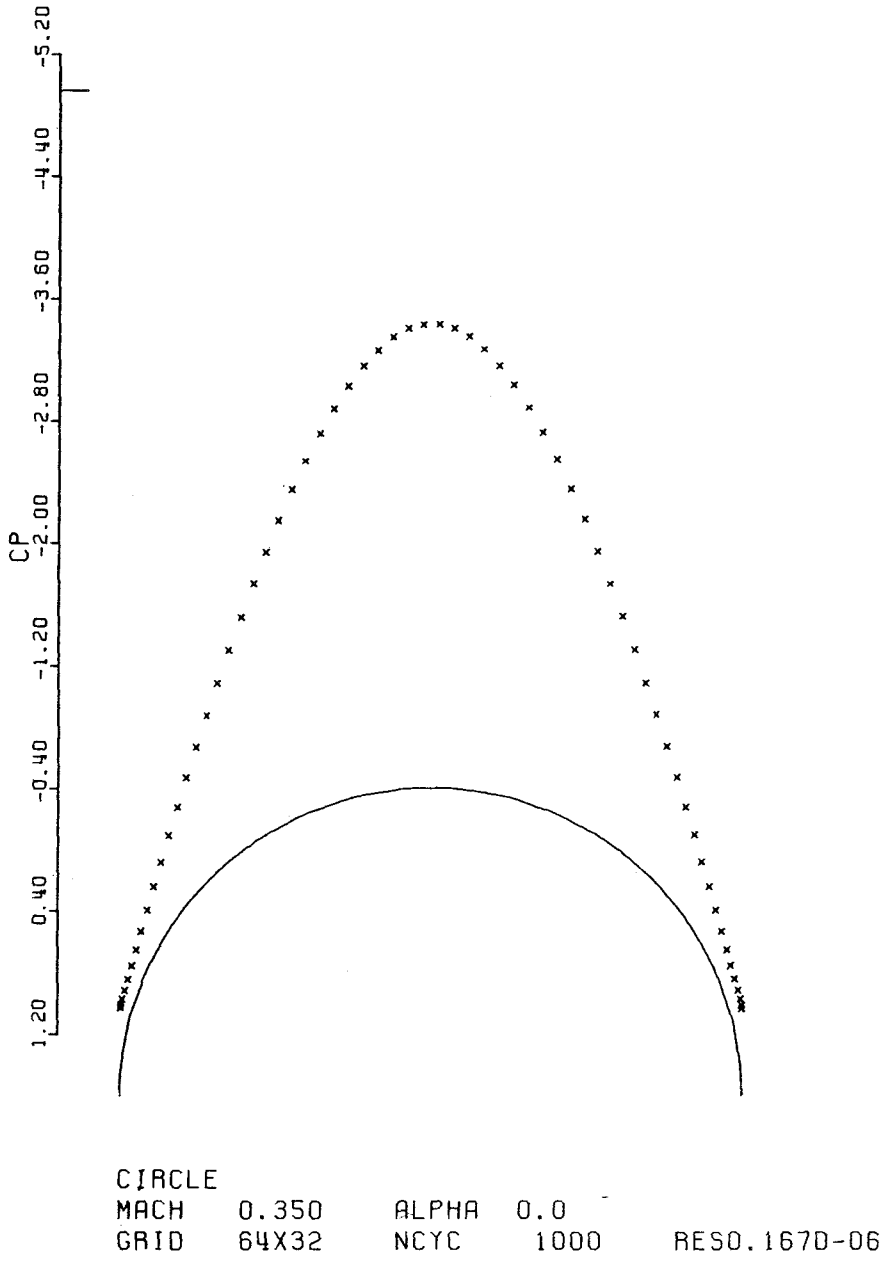

Figure 1a. Pressure Distribution of Subsonic Flow Past a Circular Cylinder

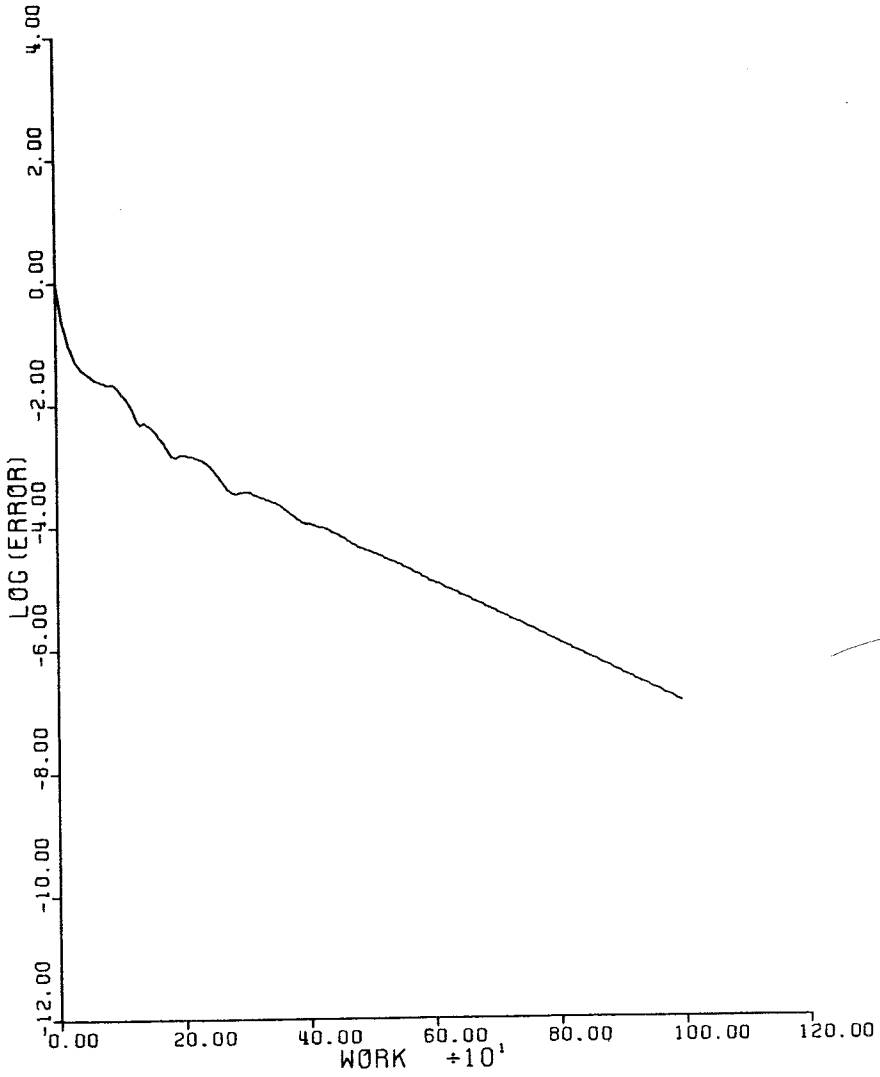

CIRCLE

MACH	0.350	ALPHA	0.0
RESID1	0.132D+01	RESID2	0.167D-06
WORK	999.00	RATE	0.9842
GRID	64X32		

Figure 1b. Convergence History for Subsonic Flow Past a Circular Cylinder

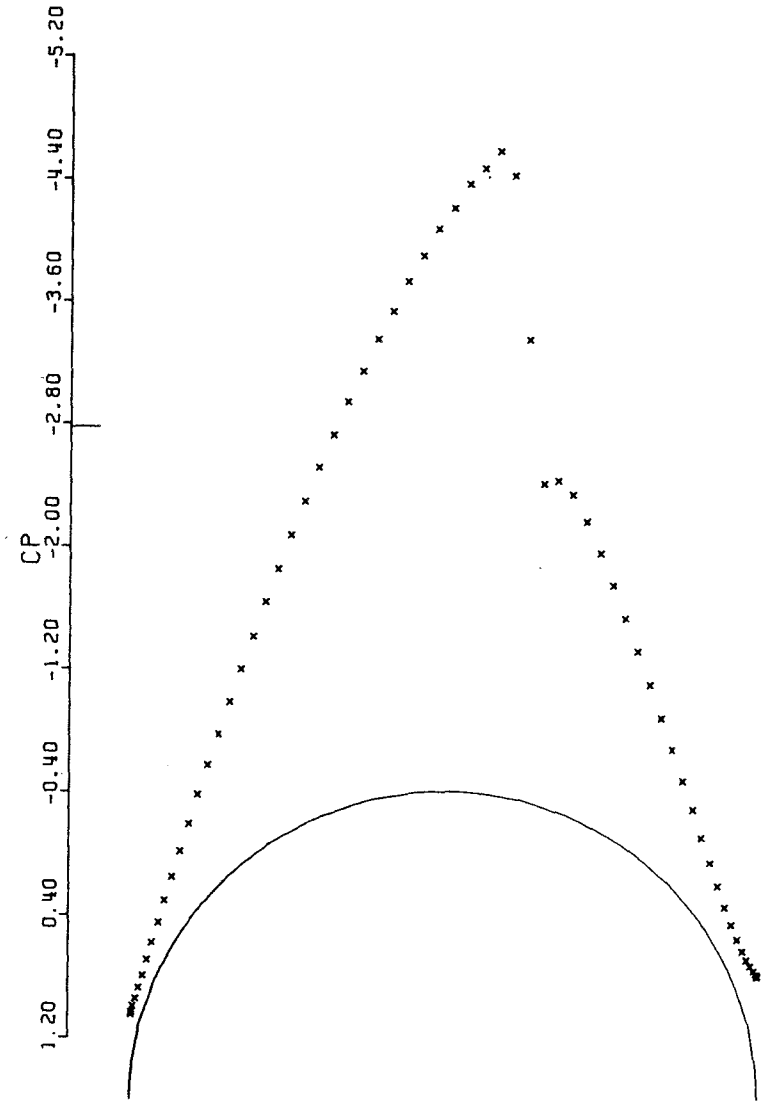

CIRCLE
MACH 0.450 ALPHA 0.0
GRID 64X32 NCYC 1000 RESO.7780-09

Figure 2a. Pressure Distribution of Transonic Flow Past a Circular Cylinder

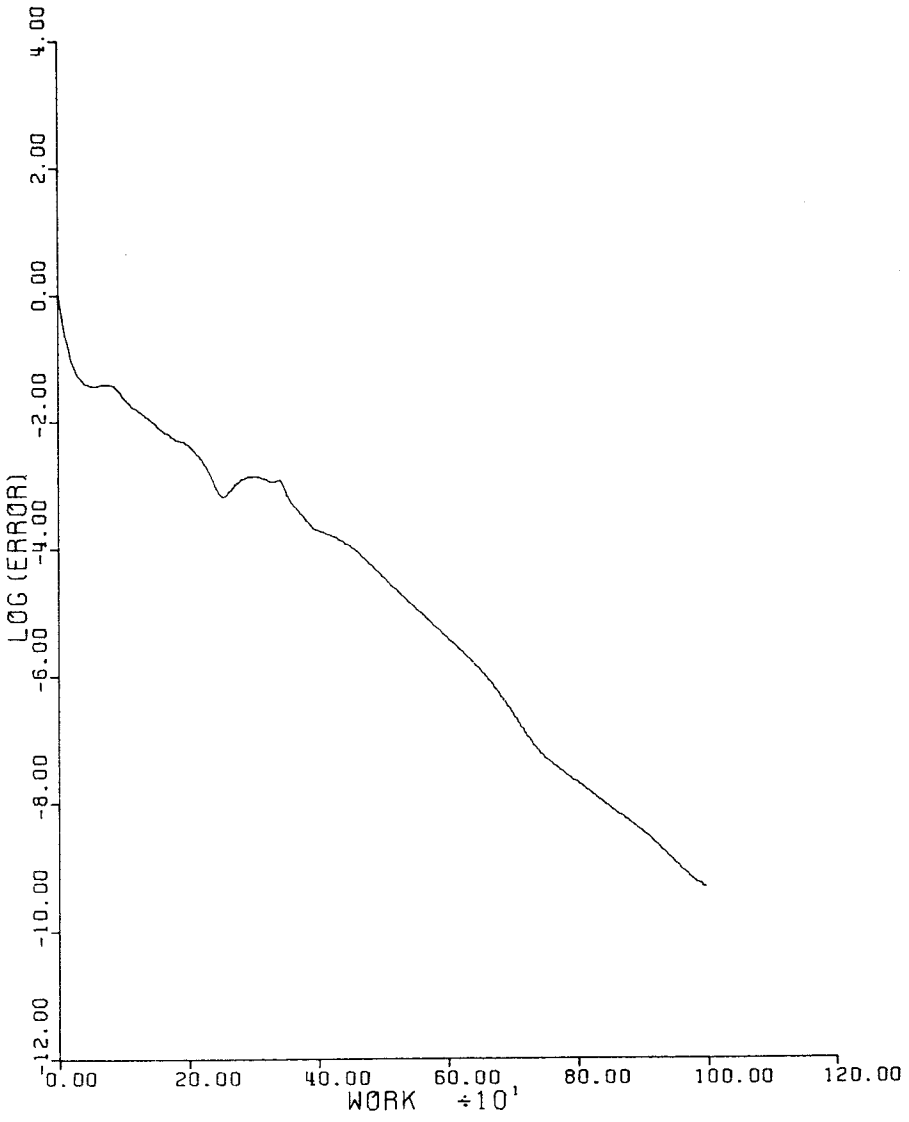

CIRCLE			
MACH	0.450	ALPHA	0.0
RESID1	0.1730+01	RESID2	0.7780-09
WORK	999.00	RATE	0.9787
GRID	64X32		

Figure 2b. Convergence History for Transonic Flow Past a Circular Cylinder

The entropy was computed to be .0120 behind the shock wave. The measure of convergence plotted in the figures is the root mean square value of $\frac{\partial \rho}{\partial t}$ (calculated as $\Delta\rho/\Delta t$ for a complete time step). In the subsonic calculation this was reduced from 1.32 to .167 10^{-6} in a 1000 cycles, with an average reduction in the error of 1.6 percent per cycle. Convergence was faster in the transonic case, at an average rate of 2.1 percent per cycle for a final error of .778 10^{-9}. Another measure of convergence is the deviation of the total enthalpy from its free stream value. The final root mean square value of this deviation was .214 10^{-6} in the subsonic calculation and .101 10^{-8} in the transonic calculation. Both calculations were performed at a fixed Courant number throughout the domain, and the enthalpy damping terms defined in Section 6 were included. The initial condition was uniform flow. The solid wall boundary condition was enforced at the first cycle, as if the cylindrical obstacle were suddenly inserted in the flow. This creates very large disturbances, but the pattern of the flow field was still established in about 400 cycles.

Figure 3 shows the result for an NACA 0012 airfoil at Mach .8 and zero degrees angle of attack. In this case the potential flow solution was calculated first and used as the initial condition for the Euler solution, allowing a comparison of the two results. The potential flow solution is shown in Figure 3a and the Euler solution in Figure 3b. It can be seen that at this Mach number the location of the shock wave is identical in the two solutions. In the Euler calculation the entropy behind the shock wave was computed to be .0053. When the Mach number is increased to .85, the entropy production through the shock wave rises to .0120 and a substantial deviation develops between the potential flow and Euler solutions, with the shock wave about 10 percent of the chord further aft in the potential flow solution. Figures 3c and 3d show

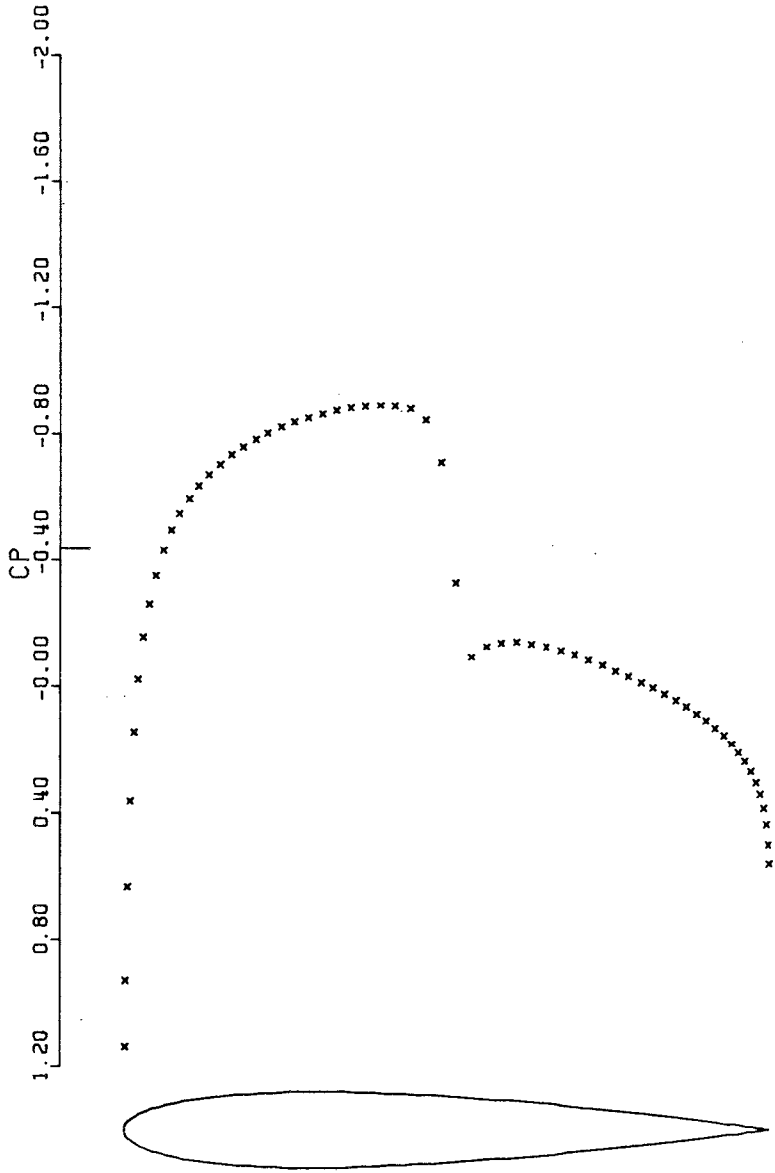

Figure 3a. Potential Flow Solution for Transonic Flow Past an NACA 0012 Airfoil

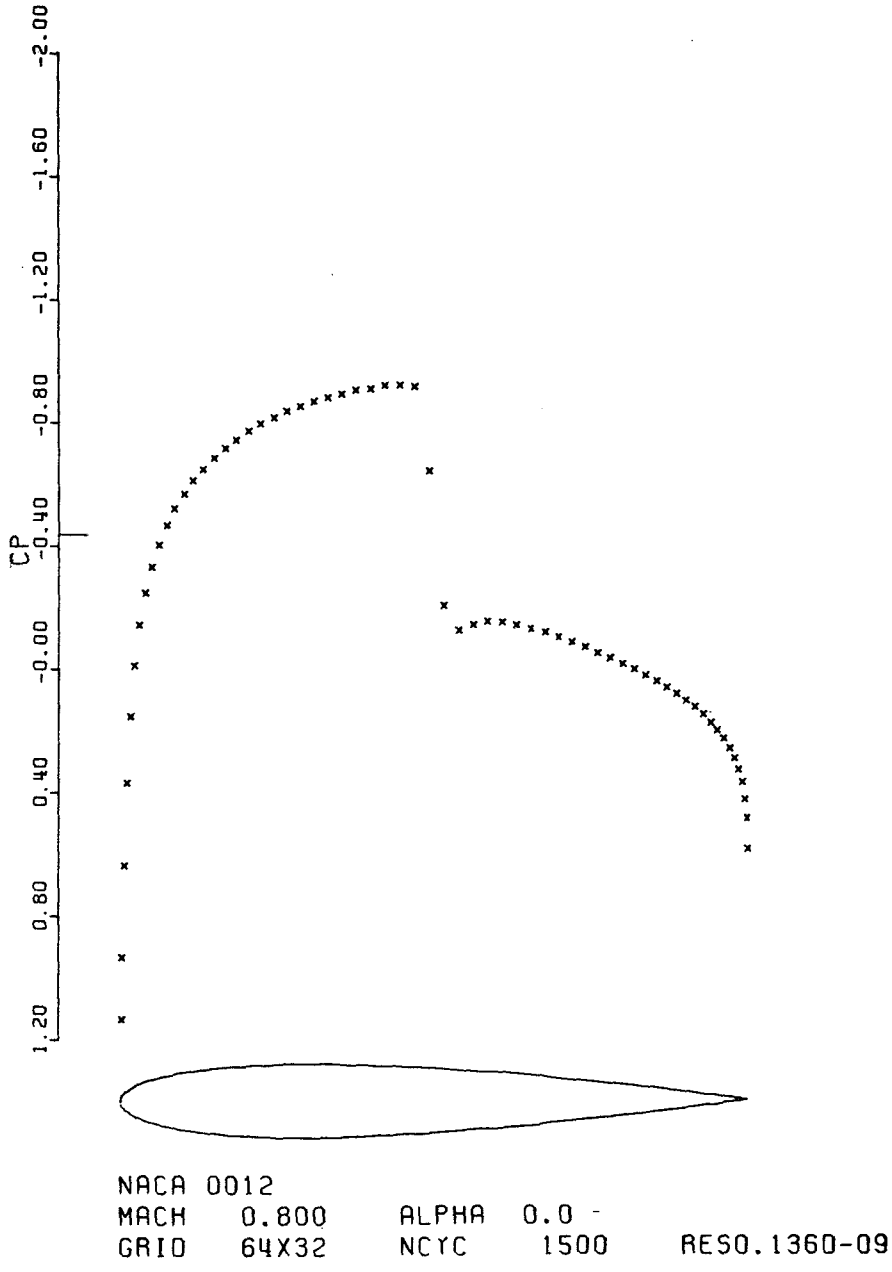

Figure 3b. Euler Solution for Transonic Flow Past an NACA 0012 Airfoil

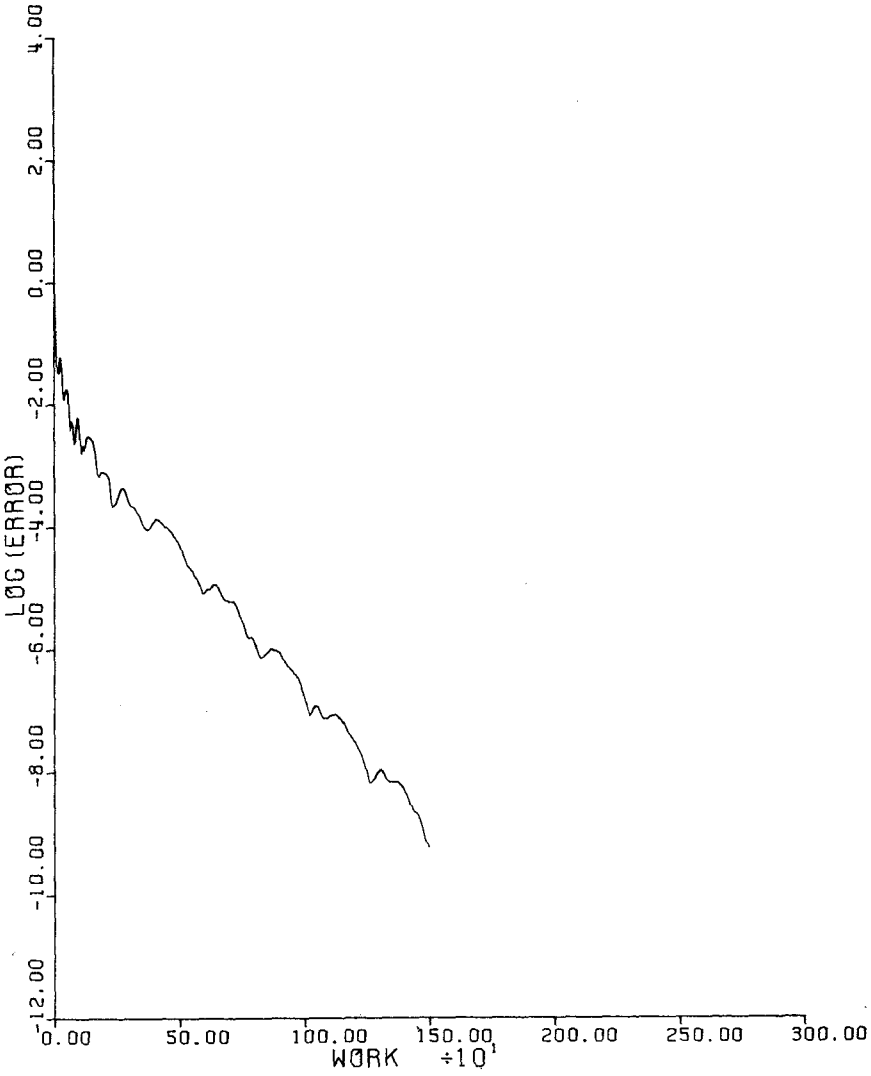

NACA 0012			
MACH	0.800	ALPHA	0.0
RESID1	0.238D+00	RESID2	0.136D-09
WORK	1499.00	RATE	0.9859
GRID	64X32		

Figure 3c. Convergence History With Enthalpy Damping

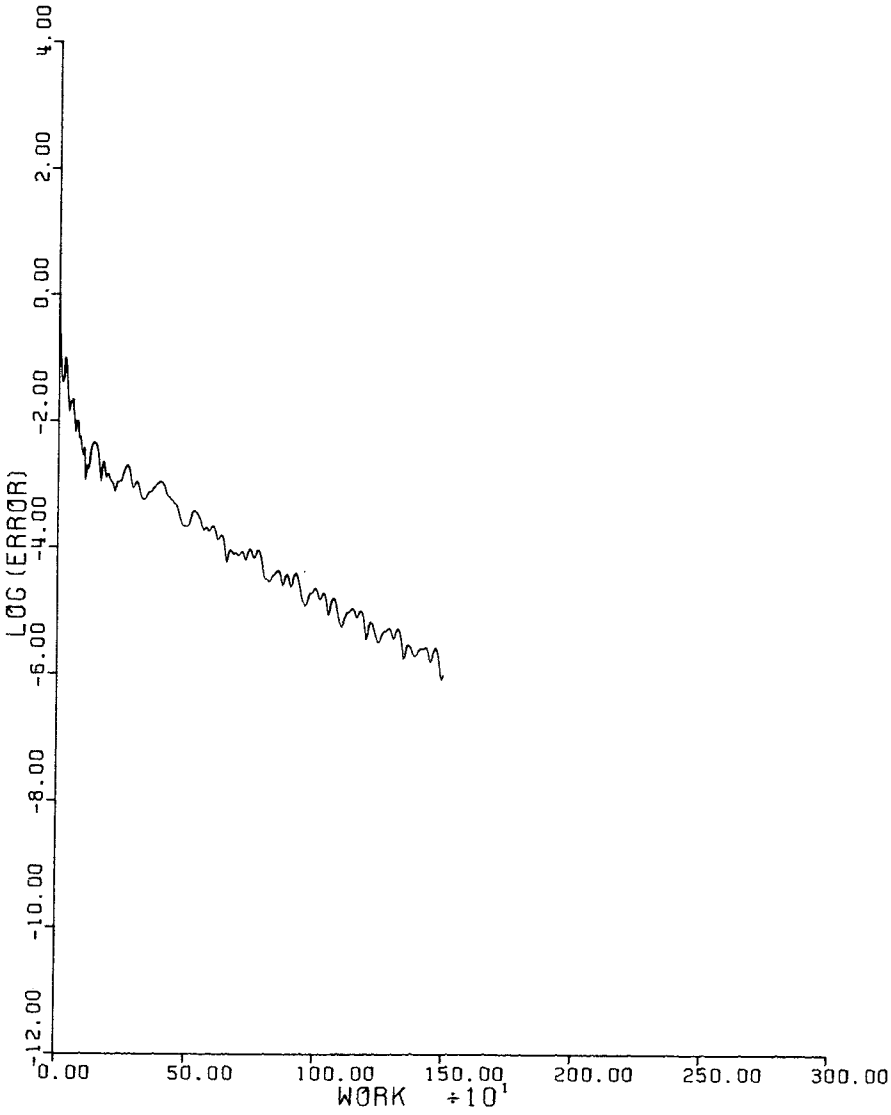

NACA 0012

MACH	0.800	ALPHA	0.0
RESID1	0.240D+00	RESID2	0.232D-06
WORK	1499.00	RATE	0.9908
GRID	64X32		

Figure 3d. Convergence History Without Enthalpy Damping

the convergence history with and without enthalpy damping. The average reduction in the error was improved from .9 percent per cycle to 1.4 percent per cycle by the enthalpy damping.

These results confirm that steady state solutions of the Euler equations can be calculated with quite moderate consumption of computer time. The present implementation of the fourth order Runge-Kutta scheme requires about 400 floating point operations at each interior cell. In a mesh with 64 x 16 = 2048 cells each cycle therefore requires about .8 megaflops (million floating point operations). The code, which is written in standard FORTRAN, runs at about 50 cycles per second on the Cray 1 computer, corresponding to a computing speed of about 40 megaflops a second. A typical run is sufficiently converged for engineering applications in 500 cycles, and requires about 10 seconds. The method has also been coded for the three dimensional flow past a swept wing. In this case about 700 floating point operations are required at each interior cell. On a mesh with 80 x 12 x 16 = 15360 cells each cycle requires about 11 megaflops, and converged results are obtained in about 500 cycles, taking about 3 1/2 minutes on the Cray 1.

References

1. Murman, E. M., and Cole, J. D.,"Calculation of Plane Steady Transonic Flows,"AIAA Journal, Vol. 9, pp. 114-121, 1971.
2. Jameson, Antony,"Iterative Solution of Transonic Flows Over Airfoils and Wings, Including Flows at Mach 1," Comm. Pure Appl. Math, Vol. 27, pp. 283-309, 1974.
3. Jameson, Antony,"Numerical Solution of Non-linear partial Differential Equations of Mixed Type," Numerical Solution of Partial Differential Equations III,

SYNSPADE 1975, edited by B. Hubbard, Academic Press, New York, 1976.

4. Jameson, Antony, and Caughey, D. A., "A Finite Volume Method for Transonic Potential Flow Calculations", Proceedings of Third AIAA Conference on Computational Fluid Dynamics, Albuquerque, 1977.
5. Rizzi, A. and Viviand, H. (editors),"Numerical Methods for the Computation of Inviscid Transonic Flow with Shocks", Proceedings of GAMM Workshop, Stockholm, 1979, Vieweg Verlag, 1981.
6. Steinhoff, J. and Jameson, A., "Multiple Solutions of the Transonic Potential Flow Equation", Fifth AIAA Computational Fluid Dynamics Conference, Palo Alto, 1981.
7. Steger, J. L., "Implicit Finite Difference Simulation of Flow about Arbitrary Geometries with Applications to Airfoils", AIAA Paper 77-665, 1977.
8. Rizzi, A., "Computation of Rotational Transonic Flow, in Numerical Methods for the Computation of Invisid Transonic Flow with Shocks", Proceedings of GAMM Workshop, Stockholm, 1979, Vieweg Verlag, 1981.
9. Viviand, H. "Pseudo Unsteady Methods for Transonic Flow Computations," Proceedings of Seventh International Conference on Numerical Methods in Fluid Dynamics, Stanford, 1980, Springer-Verlag, 1981
10. Steger, J. and Warming, R. "Flux Vector Splitting for the Inviscid Gas Dynamic Equations with Application to Finite Difference Methods", NASA TM 78605, 1979.
11. Van Leer, B., "Towards the Ultimate Conservative Differencing Scheme, V., A Second Order Sequel to Godunov's Method", J. Computational Physics, Vol. 32, pp. 101-126, 1979.

12. Beam, R. W. and Warming, R. F., "An Implicit Finite Difference Algorithm for Hyperbolic Systems in Conservation Form", J. Comp. Phys. Vol. 23, pp. 87-110, 1976.
13. Gary, J., "On Certain Finite Difference Schemes for Hyperbolic Systems", Math. Comp., Vol. 18, pp. 1-18, 1964.
14. Stetter, H. J., "Improved Absolute Stability of Predictor-Corrector Schemes", Computing, Vol. 3, pp. 286-296, 1968.
15. Graves, R. and Johnson, N.,"Navier Stokes Solutions Using Stetter's Method, AIAA Journal, Vol. 16, pp. 1013-1015, 1978.
16. Stetter, H. J., "Analysis of Discretization Methods for for Ordinary Differential Equations", Springer-Verlag, 1973.
17. Rizzi, A., "Numerical Implementation of Solid Body Boundary Conditions for the Euler Equations", ZAMM Vol. 58, pp. 301-304, 1978.
18. Kreiss, H. O., "Initial Boundary Value Problems for Hyperbolic Systems, Comm. Pure Appl. Math, Vol. 23, pp. 277-298, 1970.
19. Gottlieb, D. and Turkel, E.,"Boundary Conditions for Multistep Finite Difference Methods for Time Dependent Equations", J. Computational Physics, Vol. 26, pp. 181-196, 1978.
20. Gustafsson, B. and Oliger, J.,"Stable Boundary Approximations for a Class of Time Discretizations of $u_t=AD_o u$,", Upsala University, Dept. of Computer Sciences, Report 87, 1980.
21. Rudy, D. and Strikwerda, J., "A Non-reflecting Outflow Boundary Condition for Subsonic Navier Stokes Calculations", J. Computational Physics, Vol. 36, pp. 55-70, 1980.
22. Garabedian, P. R., "Estimation of the Relaxation Factor for Small Mesh Size", Math Tables Aids Comp., Vol. 10, pp. 183-185, 1956.